

One-dimensional GaN nanomaterials transformed from one-dimensional Ga₂O₃ and Ga nanomaterials

X. Y. Han¹, Y. H. Gao^{1,2,*} and X. H. Zhang¹

One-dimensional (1D) GaN nanomaterials exhibiting various morphologies and atomic structures were prepared via ammoniation of either Ga₂O₃ nanoribbons, Ga₂O₃ nanorods or Ga nanowires filled into carbon nanotubes (CNTs). The 1D GaN nanomaterials transformed from Ga₂O₃ nanoribbons consisted of numerous GaN nanoplatelets having the close-packed plane, i.e. (0002)_{2H} or (111)_{3C} parallel to the axes of starting nanoribbons. The 1D GaN nanomaterials converted from Ga₂O₃ nanorods were polycrystalline rods covered with GaN nanoparticles along the axes. The 1D GaN nanomaterials prepared from Ga nanowires filled into CNTs displayed two dominant morphologies: (i) single crystalline GaN nanocolumns coated by CNTs, and (ii) pure single crystalline GaN nanowires. The cross-sectional shape of GaN nanowires were analyzed through the transmission electron microscopy (TEM) images. Formation mechanism of all-mentioned 1D GaN nanomaterials is then thoroughly discussed.

Keywords: GaN; One-dimensional; Ga₂O₃; Nanostructures

Citation: X. Y. Han, Y. H. Gao and X. H. Zhang, "One-dimensional GaN nanomaterials transformed from one-dimensional Ga₂O₃ and Ga nanomaterials", Nano-Micro Lett. 1, 4-8 (2009). [doi: 10.5101/nml.v1i1.p4-8](https://doi.org/10.5101/nml.v1i1.p4-8)

GaN is a wide direct-bandgap (3.39 eV at room temperature) semiconductor material and its one-dimensional (1D) structure has a high potential for applications in blue and UV light-emitting and laser diodes as well as in high temperature and high power electronic devices [1,2]. Up to date, the synthetic approaches for 1D GaN nanomaterials have relied on various physical or chemical methods, such as carbon nanotubes (CNTs) [3-5] and anodic alumina membrane [6,7] template-originated methods, Fe, Co, Ni and Au metal-catalyst vapor-liquid-solid (VLS) growth [8-10], SiO₂, Fe₂O₃, and B₂O₃ oxide-assisted growth (OAG) [11,12], Precursor-based methods metalorganic chemical vapor deposition (MOCVD) [13], and hydride vapor phase epitaxy (HVPE) [14].

Although the above-mentioned groups are different from each another, all methods are capable of generating 1D GaN nanomaterials with a characteristic single-crystalline structure.

Liliental-Weber [15] and Lan [16] have reported preferentially-oriented 1D GaN nanomaterials consisting of small GaN platelets. Furthermore, Zhao [17] and Ogi [18] have studied the influence of starting materials Ga₂O₃ powders (particles) on growth of GaN nanomaterials. Though the formation mechanism of the GaN nanomaterials has been discussed, the reason behind the orientated growth remains unclear. Our current investigation sheds an additional light on this issue. In addition, the design, synthesis, and characterization of surface-modified nanostructures are of fundamental importance in controlling the mesoscopic properties of new materials and in developing new tools for nanofabrication. So we expect that presently synthesized GaN 1D nanomaterials coated with GaN nanoparticles are capable of bringing new electronic characteristics different from those displaying by their simple mechanical mixtures due to somewhat specific boundary

¹Wuhan National Laboratory for Optoelectronics-School of Physics, Huazhong University of Science and Technology, Wuhan 430074, China

²Wuhan National Laboratory for Optoelectronics & College of Optoelectronic Science and Engineering, Huazhong University of Science and Technology, Wuhan 430074, China

*Corresponding author. Email: gaoyihua@mail.hust.edu.cn. Telephone: +86-027-87792242-806

electron conditions.

GaN nanoribbons consisting of platelets were fabricated in a conventional furnace with a horizontal quartz tube. Ga and Ga₂O₃ powders were homogeneously mixed in a weight ratio 1:1. The mixture was placed in a BN crucible and covered by a BN plate with drilled mm-size channels. Bundles of CNTs were placed on the BN plate. The synthesis process was performed in two steps. First, the furnace was washed with a N₂ gas (3 l/min) over ~2 hours under gradual heating to 900°C. Second, a mixture of NH₃ (0.3 l/min) and N₂ (1 l/min) was substituted for the original N₂ gas flow while the temperature was gradually increased to 970°C over 10 min and then kept constant during 30 min. Then, the whole quartz tube was taken out from the furnace and cooled to the room temperature. We found that the surface of the starting CNTs was covered with a thin layer of yellow-colored material.

Firstly, Ga₂O₃ nanorods and Ga-filled CNTs were synthesized in a vertical radio-frequency furnace by mixture of Ga₂O₃ and pure amorphous active carbon. (see also Refs. [19, 20]) The furnace was heated at 1360°C over 1-2 h. Ga-tipped Ga₂O₃ nanorods were found to be deposited on the outer surface of the C fiber coat where the temperature was estimated to be approximately 1000°C. Meanwhile, Ga-filled CNTs were collected from the inner surface of the outlet pipe of the furnace where the temperature was estimated to be ~800°C. Then, place Ga₂O₃ nanorods and Ga-filled CNTs into the conventional furnace for ammoniation at 970°C (described above), respectively. Finally all the resultant materials were collected and studied by a 300 kV field emission analytical high-resolution transmission electron microscope (HRTEM, JEM-3000 F) equipped with an X-ray energy dispersive spectrometer (EDS).

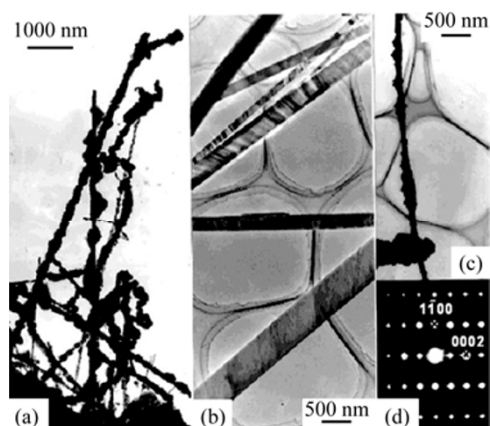


FIG. 1. (a) Morphology of the yellow-colored materials synthesized in a NH₃ atmosphere. (b) Morphology of the white-colored materials synthesized in a N₂ atmosphere. (c) A GaN nanoribbon transformed from a Ga₂O₃ ribbon and its [1120] diffraction pattern in (d).

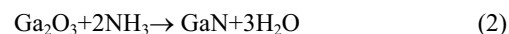
Figure 1(a) depicts the morphology of the yellow-colored materials synthesized via a reaction Ga and Ga₂O₃ powders with NH₃. They have widths of 40-100 nm and lengths of up to 10 μm. The materials were detected to be 1D nanoribbons consisting of numerous nanoplatelets. An energy dispersion spectroscopy (EDS) analysis indicated that the nanoribbons are composed of Ga and N. It is believed that two processes are involved in the growth of the nanoribbons: (i) Ga₂O₃ nanoribbons are crystallized on the surface of CNTs, and, while a N₂ gas having impurities of O₂, is introduced into the furnace, the chemical reactions proceed as follows:



where a Ga₂O vapor is generated in line with the reaction described by Han et al [3].



The vapor cannot be oxidized further after it reaches the surface of CNTs, because the CNTs serve as a shelter for the O₂ impurity in N₂ gas; (ii) Ga₂O₃ nanoribbons are transformed into GaN nanoribbons while NH₃ is introduced into the furnace; the involved reaction may be written as follows,



where GaN platelets may initially nucleate on the side-surface of a Ga₂O₃ nanoribbon and the subsequent growth of GaN platelets propagates along the whole nanoribbon.

To confirm the growth mechanism of the yellow-colored Ga₂O₃ nanoribbons, we carried out additional experiments. Before the second step, we examined a thin layer of the white-colored materials on the surface of CNTs. The materials were determined to be Ga₂O₃ nanoribbons having morphologies depicted in Fig. 1(b). After ammoniation of the Ga₂O₃ nanoribbons at 970°C, we found that the color of the materials was changed from white to yellow. The later materials were

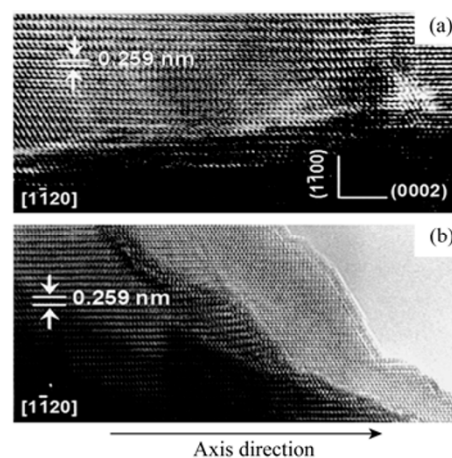


FIG. 2. (a) [1120] HRTEM image of a platelet on a nanoribbon in Fig. 1(a), and (b) [1120] HRTEM image of a platelet on the nanoribbon in Fig. 1(c). There is a common characteristic in the two images: a thicker GaN platelet is under a thinner GaN platelet with the (0002)_{2H} stacking plane.

found to be GaN. There were nanoribbons covered with nano-platelets. A nanoribbon is shown in Fig. 1(c), its axis is parallel to the (0002) plane, as shown in Fig. 1(d), which is the $[11\bar{2}0]$ zone axis diffraction pattern. The similarity between the morphologies in Fig. 1(a) and Fig. 1(c) suggests that the proposed growth mode for the nanoribbons depicted in Fig. 1(a) is correct. The reasonability of the proposed growth mode may require other evidence additive to the fact of similar morphologies of the two kinds of the GaN nanoribbons. Detailed HRTEM investigation may become effective.

Figure 2(a) and (b) are the $[11\bar{2}0]$ HRTEM images of two platelets on a nanoribbon in Fig. 1(a) and that in Fig. 1(c), respectively. The two images have one characteristic in common - a thicker GaN platelet laying under a thinner GaN platelet with the (0002)_{2H} stacking plane. Figure 3(a) and (b), $[1\bar{1}0]$ HRTEM images of two platelets on a nanoribbon in Fig. 1(a) and that in Fig. 1(c), also showing that a thicker GaN

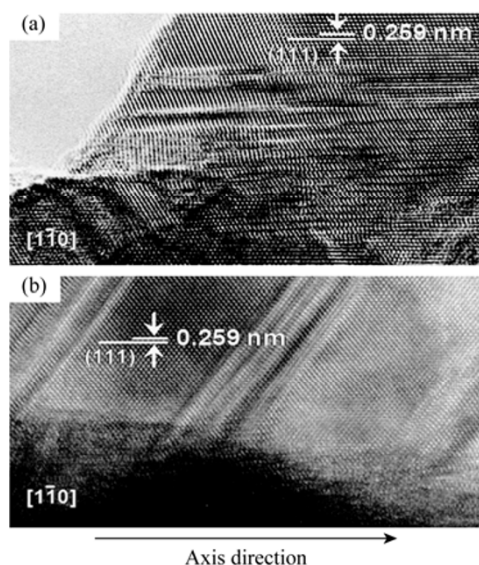


FIG. 3. (a) $[110]$ HRTEM image of a platelet on the nanoribbon in Fig. 1(a), and (b) $[110]$ HRTEM image of a platelet on the nanoribbon Fig. 1(c). There is also a common characteristic in two images: a thicker GaN platelet is under a thinner GaN platelet with the (111)_{3C} stacking plane.

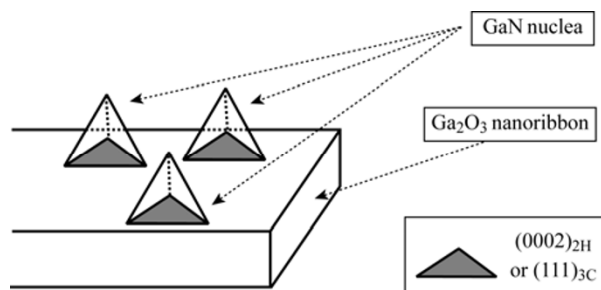


FIG. 4. A schematic of Ga₂O₃ to GaN conversion during an initial transformation stage. GaN nucleates on a side surface of a nanoribbon with its close-packed plane stacked to the side surface of a certain plane, resulting in the axis parallel to the stacking plane.

platelet is under a thinner GaN platelet with the (111)_{3C} stacking plane. In the four HRTEM images, the close-stacking (0002) and/or (111) planes are parallel to the axis direction of the nanoribbons. The relationship can be explained in terms of the growth mode schematic of GaN nucleation shown in Fig. 4. When GaN islands nucleate on a certain side surface of a Ga₂O₃ nanoribbon, their close packing planes stack to the side surface of a certain plane, resulting in the axis parallel to the stacking plane.

Figure 5(a) shows the morphology of Ga-tipped Ga₂O₃ nanorods, which were found to have a round cross-section under tilting experiments in TEM. After ammoniation, the Ga₂O₃ nanorods and their spherical tips were transformed to GaN nanorods with spherical GaN tips. Generally the rods were covered by numerous nanoparticles, as shown in Fig. 5(b) and 5(c), respectively. The GaN nanorods were polycrystalline and have no preferred axis direction. These nanorods are different from the GaN nanoribbons converted from Ga₂O₃ nanoribbons, which have a definite axis direction parallel to the (0002)_{2H} and/or (111)_{3C} planes. The origin of this phenomenon can be

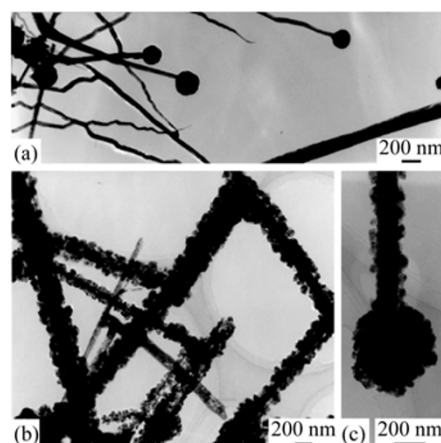


FIG. 5. (a) Morphology of Ga-tipped Ga₂O₃ nanorods. (b) Morphology of GaN nanorods consisting of numerous GaN nanoparticles on their surface. (c) Morphology of a spherical GaN tip consisting of numerous GaN nanoparticles.

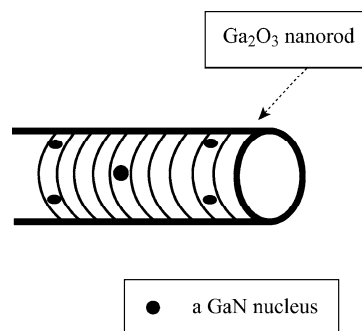


FIG. 6. A schematic of an initial stage of transformation from a Ga₂O₃ to a GaN nanorod. GaN randomly nucleates on the round side surface at numerous sites, resulting in a GaN nanorod with numerous particles.

explained through a schematic diagram, Fig. 6. During the transformation, randomly-oriented GaN domains nucleate on a round side surface at numerous sites finally resulting in a polycrystalline GaN nanorod.

Figure 7(a) depicts the morphology of a Ga nanowire filled into CNT. After ammoniation, a Ga nanowire can be transformed to GaN nanocolumns coated by CNTs, as shown in Fig. 7(b). Figure 7(c) and d are the EDS spectra taken from the pre- and post-transformed Ga nanowires, respectively. HRTEM study illustrates that each GaN nanocolumn is single crystalline. Figure 7(e) shows a HRTEM image of such single-crystalline GaN nanocolumn coated by C layers.

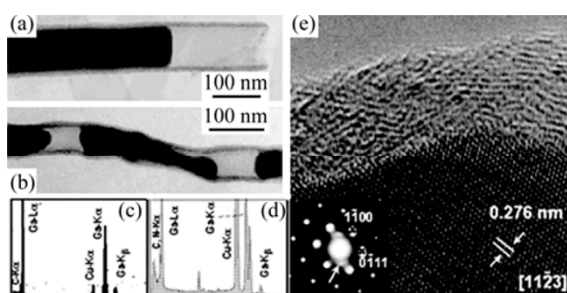


FIG. 7. (a) Morphology of a Ga nanowire filled in CNT. (b) Morphology of GaN nanocolumns coated by CNTs and transformed from a Ga nanowire filled into CNT. (c) and (d) EDS spectra of a Ga nanowire and a GaN column filled in CNT, respectively. (e) HRTEM image of a GaN column filled in a CNT.

The formation of GaN nanowires filled in CNTs can be explained as direct ammoniation of Ga nanowires filled in CNTs. However, such explanation may find a better proof if a pure GaN nanorod not covered with a CNT may be found in the ammonia-treated materials. In fact, such material was found, as shown in Fig. 8(a). This rod has an axis perpendicular to the $(1\bar{1}00)$ plane, as displayed in Fig. 8(b) and (c). The most intriguing fact is that new contrast fringes appear in Fig. 8(a). It is believed that the fringes are originated from the thickness difference [21]. According to this, we can conjecture that the cross-section of the rod may have two kinds of possible shapes shown in Fig. 9. The above-presented analysis made us possible to estimate the thickness and the cross-section shape using the observed contrast fringes. It is noted though that a more definite confirmation using a slice method of cross-section is probably needed [22].

The formation of a pure GaN nanorod can also be explained due to ammoniation of Ga in CNTs. When a metallic Ga with a density of $\sim 5.90 \text{ g/cm}^3$ is gradually transformed to GaN with a density of $\sim 5.90 \text{ g/cm}^3$, the volume increased by 20% as the molecular weight increased by 20%. This extra volume part gradually grows and leads to a resultant pure GaN

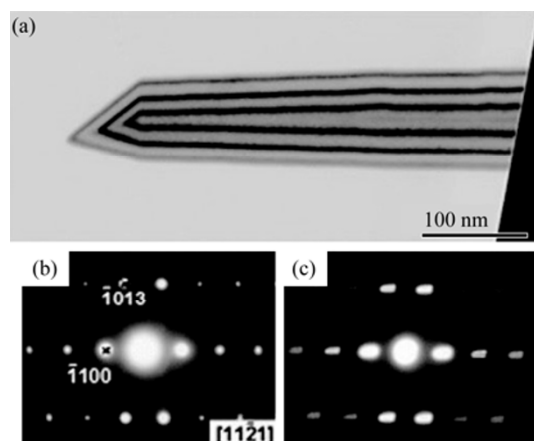


FIG. 8. (a) TEM image of a pure GaN nanorod. (b) and (c), diffraction patterns focus and defocus $[11\bar{2}1]$ zone axis, respectively, which show that the GaN can be indexed as 2H structure with its axis along $[1\bar{1}00]$ direction.

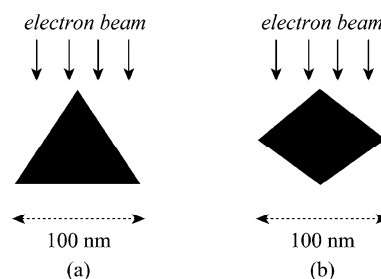


FIG. 9. Two kinds of possible cross-sectional shapes of the pure GaN nanowire in Fig. 8(a).

nanorod whose cross-section may become non-round as compared to a round shape of the initial Ga nanorod.

To sum up, the presented transformation scheme consists of two steps and relies on conversion of a given 1D material to another 1D material in a given gaseous atmosphere. This approach has been used to synthesize ZnS [23] and GaN nanotubes [24, 25]. It is believed here that the process is an important practical method to synthesize novel 1D material and to fabricate complicated arrays of those with nanoparticles.

We fabricated one-dimensional GaN nanoribbons, nanorods, and nanowires through ammoniation of Ga_2O_3 nanoribbons, Ga_2O_3 nanorods and Ga nanowires filled in CNTs, respectively. The GaN nanoribbons consist of numerous GaN nanoplatelets with the close-packed planes, i.e. $(0002)_{2\text{H}}$ or $(111)_{3\text{C}}$ being in parallel with the axis of nanoribbons. The GaN nanorods obtained from Ga_2O_3 nanorods are polycrystalline nanorods attaching numerous GaN nanoparticles along their axes. GaN nanowires coated with CNT layers were single-crystalline. The thickness and cross-sectional shape of a pure GaN nanowire may be calculated and conjectured according to the thickness fringes in its transmission electron

microscopy image. Formation mechanisms of 1D GaN nanomaterials are believed to be governed through inhering corresponding 1D characteristics of the starting Ga₂O₃ and Ga materials, whereas the nucleation during initial transformation stage may result in new nanoparticle formation.

Thanks to the National Natural Science Foundation of China (No.10774053), Hubei Province Nature Science Foundation of China (No.2007ABB008) and Programs Foundation of Ministry of Education of China (No. 20070487038).

Received 18 August 2009; accepted 30 August 2009; published online 15 October 2009.

References

1. J. Pankove and T. Moustakas, Gallium Nitride (GaN), Semiconductors and Semimetals, Academic Press, San Diego, 1998.
2. H. W. Seo, L. W. Tu, Y. T. Lin, C. Y. Ho, Q. Y. Chen, L. Yuan, D. P. Norman and N. J. Ho, Appl. Phys. Lett. 94, 201907 (2009). [doi:10.1063/1.3129191](https://doi.org/10.1063/1.3129191)
3. W. Q. Han, S. S. Fan, Q. Q. Li and Y. D. Hu, Science 277, 1287 (1997). [doi:10.1126/science.277.5330.1287](https://doi.org/10.1126/science.277.5330.1287)
4. X. Duan and C. M. Lieber, J. Am. Chem. Soc. 122, 188 (2000). [doi:10.1021/ja993713u](https://doi.org/10.1021/ja993713u)
5. W. Q. Han and A. Zettl, Adv. Mater. 14, 1560 (2002). [doi:10.1002/1521-4095\(20021104\)14:21<1560::AID-ADMA1560>3.0.CO;2-P](https://doi.org/10.1002/1521-4095(20021104)14:21<1560::AID-ADMA1560>3.0.CO;2-P)
6. G. S. Cheng, L. D. Zhang, Y. Zhu, G. T. Fei, L. Li, C. M. Mo and Y. Q. Mao, Appl. Phys. Lett. 75, 2455 (1999). [doi:10.1063/1.125046](https://doi.org/10.1063/1.125046)
7. L. X. Zhao, G. W. Meng, X. S. Peng, X. Y. Zhang and L. D. Zhang, J. Crystal Growth 235, 124 (2002). [doi:10.1016/S0022-0248\(01\)01836-X](https://doi.org/10.1016/S0022-0248(01)01836-X)
8. X. F. Duan and C. M. Lieber, J. Am. Chem. Soc. 122, 188 (2000). [doi:10.1021/ja993713u](https://doi.org/10.1021/ja993713u)
9. X. H. Chen, J. Xu, R. M. Wang and D. P. Yu, Adv. Mater. 15, 419 (2003). [doi:10.1002/adma.200390097](https://doi.org/10.1002/adma.200390097)
10. X. T. Zhou, T. K. Sham, Y. Y. Shan, X. F. Duan, S. T. Lee and R. A. Rosenberg, J. Apply. Phys. 97, 104315 (2005).
11. R. Q. Zhang, Y. Lifshitz and S. T. Lee, Adv. Mater. 15, 635 (2003). [doi:10.1002/adma.200301641](https://doi.org/10.1002/adma.200301641)
12. S.Y. Bae, H. W. Seo, J. Park, H. Yang, J. C. Park and S. Y. Lee, Appl. Phys. Lett. 81, 126 (2002). [doi:10.1063/1.1490395](https://doi.org/10.1063/1.1490395)
13. F. Qian, Y. Li, S. Gradecak, D. Wang, C. J. Barrelet and C. M. Lieber, Nano Lett. 4, 1975 (2004). [doi:10.1021/nl0487774](https://doi.org/10.1021/nl0487774)
14. H. M. Kim, D. S. Kim, Y. S. Park, D. Y. Kim, T. W. Kang and K. S. Chung, Adv. Mater. 14, 991 (2002).
15. Z. Liliental-Weber, Y. H. Gao and Y. Bando, J. Elec. Mater. 31, 391 (2002).
16. Z. H. Lan, C. H. Liang, C. W. Hsu, C. T. Wu, H. M. Lin, S. Dhara, K. H. Chen, L. C. Chen and C. C. Chen, Adv. Funct. Mater. 14, 233 (2004). [doi:10.1002/adfm.200304403](https://doi.org/10.1002/adfm.200304403)
17. M. Zhao, X. L. Chen, W. J. Wang, Z. H. Zhi and Y. P. Xu, Chin. Phys. Lett. 24, 401 (2007).
18. T. Ogi, Y. Kaihatsu, F. Iskandar, E. Tanabe and K. Okuyama, Adv. Powder. Tech. 20, 29 (2009).
19. Y. H. Gao, Y. Bando, T. Sato, Y. F. Zhang and X. Q. Gao, Appl. Phys. Lett. 81, 2267 (2002). [doi:10.1063/1.1507835](https://doi.org/10.1063/1.1507835)
20. Y. H. Gao and Y. Bando, Nature 415, 599 (2002). [doi:10.1038/415599a](https://doi.org/10.1038/415599a)
21. P. B. Hirsch, I. Howie, R. B. Nicholson and D. W. Pashley, Electron Microscopy of Thin Crystals (Butterworths Co. LTD, London, 1965) pp. 159.
22. J. Q. Hu, Q. Li, N. B. Wong, C.S. Lee and S. T. Lee, Chem. Mater. 14, 1216 (2002). [doi:10.1021/cm0107326](https://doi.org/10.1021/cm0107326)
23. X. D. Wang, P. X. Gao, J. Li, C. J. Summers and Z. L. Wang, Adv. Mater. 14, 1732 (2002). [doi:10.1002/1521-4095\(20021203\)14:23<1732::AID-ADMA1732>3.0.CO;2-5](https://doi.org/10.1002/1521-4095(20021203)14:23<1732::AID-ADMA1732>3.0.CO;2-5)
24. J. Q. Hu, Y. Bando, D. Golberg and Q. L. Liu, Angew. Chem. Int. Ed. 42, 3493 (2003). [doi:10.1002/anie.200351001](https://doi.org/10.1002/anie.200351001)
25. J. Dinesh, M. Eswaramoorthy and C. N. R. Rao, J. Phys. Chem. C. 111, 510 (2007). [doi:10.1021/jp0674423](https://doi.org/10.1021/jp0674423)